

# Percolation upon expansion of nanosecond-pulse-produced laser plasma into a gas

N.E. Kask, S.V. Michurin, G.M. Fedorov

**Abstract.** Spectral studies of a plasma expanding into the ambient gas upon ablation of various targets by nanosecond laser pulses of moderate intensities are performed. It is found that the dependences of the intensities of spectral lines on the pressure of the buffer gas and the target composition have a threshold character typical of percolation. It is ascertained that a three-dimensional percolation occurs in plasma, and its threshold is determined by the atomic density of the metal component contained in the target. It is shown that percolation clusters, existing at temperatures higher than the boiling temperature of the target material, affect the plasma absorption ability, temperature, and spectral continuum of plasma emission.

**Keywords:** laser ablation, laser plasma, percolation.

## 1. Introduction

According to [1, 2], a finely dispersed condensed phase—compact clusters, fractal aggregates, and small droplets of a melt—plays the main role in the absorption of laser radiation by a low-temperature plasma plume in the case of millisecond laser pulses. The brightness temperature of radiation from condensed particles cannot be higher than the boiling temperature of the target material. However, if plasma expands into a gas whose pressure exceeds a certain critical value characteristic of the target material, the effective temperatures of a light flash appreciably exceed the boiling temperature of the condensate [3]. The shape and size of the plasma region change in this case. As the density of the number of condensed particles in the plasma increases, the interaction between them becomes so strong that a transition from the gas plasma to a plasma droplet occurs. For a plasma produced upon evaporation of targets by millisecond laser pulses, a macroscopic fractal shell forms in the peripheral layers of the plasma [4].

As was shown in [5], the relationship between the magnetic-dipole and electric-dipole absorptions of microwave radiation in a laser plasma plume most adequately

corresponds to the model of a fractal (in particular, percolation) cluster. The fractal dimension of the latter depends on the dimension of the Euclidean space, while the cluster size is determined by the dimensions of the region under study. If the model of microscopic percolation is realised or the fractal cluster consists of virtual chains (gaslike structures with a minimum number of bonds between atoms [6]), then, in contrast to compact clusters, such structures do not disappear when the boiling temperature of the material is exceeded. The condition for their existence reduces to the fact that the medium density must be higher than a certain critical value. Percolation must also occur upon ablation of targets produced by short laser pulses, since, the higher the light flux intensity, the denser the near-surface plasma produced. Experimental studies of a plasma produced by nanosecond laser pulses are complicated by plasma degradation processes and the requirements of a high temporal resolution of the recording instruments. An alternative way to study the clusterisation process is offered by the techniques developed to study the percolation in a laser plasma plume near the surfaces of composite targets [7] and the spectral properties of the plasma emission continuum [3].

The dynamics of plasma expansion into the ambient gas, the plasma composition, and different processes proceeding in it, such as the absorption of laser radiation, heating, ionisation, recombination, condensation, and clusterisation, depend, in particular, on the external pressure of the ambient gas. According to [8], at pressures below  $10^{-5}$  atm, a free adiabatic plasma expansion takes place. Collisions of plasma particles with atoms of the ambient (buffer) gas begin to affect the process at pressures of  $\sim 10^{-4}$  atm, when an appreciable increase in the plume emission intensity is observed 1–2  $\mu$ s after the end of a laser single pulse. In the case of plasma expansion into vacuum upon ablation of Al [8] and Si [9] targets, it follows from the ratio of the intensities of ion lines that the plasma temperature reaches a maximum ( $\sim 10^4$  K) at the end of a single pulse and then falls at a characteristic time of  $\sim 10^{-7}$  s. It is obvious that the subsequent increase in the flash intensity observed several microseconds after the plasma expansion into the ambient gas is a consequence of a change in its emission (or absorption ability) as a result of condensation and clusterisation processes. According to [10], during laser ablation in the buffer gas at atmospheric pressure, a spherical plasmoid forms near the target and emits radiation that decays at a characteristic time of tens of microseconds. Such a slow plasma relaxation results from an energy released in the three-body recombination process. It is

---

N.E. Kask, S.V. Michurin, G.M. Fedorov D.V. Skobel'tsyn Institute of Nuclear Physics, Moscow State University, Vorob'evy gory, 119992 Moscow, Russia; e-mail: nek@srd.sinp.msu.ru

Received 27 September 2004

Kvantovaya Elektronika 35 (1) 48–52 (2005)

Translated by A.S. Seferov

---

known from experiments [9, 11] that the intensities of discrete spectral lines and molecular bands belonging to ions and dimers of the evaporated substance, respectively, correlate with the efficiency of the formation of nanoparticles in the condensate. Ions polarise vapour atoms by their field and attract them, thereby being centres of heterogeneous nucleation [9], while, according to [6], dimers are the main elements in gaslike clusters.

This paper presents the results of an experimental study of the emission of a short-lived plasma appearing upon ablation of various substances by nanosecond pulses, depending on the target composition and external pressure produced by the ambient gas. The components composing the laser plasma were determined from the intensities of atomic and ion discrete spectra, molecular bands, and continuum. As was shown in our earlier works [3, 4, 7], the intensity of a continuous emission spectrum correlates, depending on the target composition, with the threshold behavior of the high-frequency conductivity of laser plasma, which is typical of percolation, and with the appearance of microstructures of fractal nature.

## 2. Experimental

Ablation of targets was performed by 10-mJ, 10-ns single pulses from a 1.06- $\mu\text{m}$  Nd:YAG laser. The laser power density in the irradiated spot was  $\sim 10^8 \text{ W cm}^{-2}$ . The spectral unit of the setup was described in [3]. Spectra of the laser plasma produced near the surface of metals and binary targets (powder mixtures and alloys) were studied. Powder mixtures were melted in an electric arc between tungsten electrodes in an argon atmosphere at normal pressure. The target was placed in a hermetically sealed chamber that allowed studies of the laser plume at buffer-gas pressures of 0.001–100 atm.

Test experiments with repeated irradiation helped to choose optimal surface-irradiation conditions based on the reproducibility of the signal under study for two sequential pulses. These were the first and second pulses for metals and alloys and second and third pulses for a powder mixture, after which the target was displaced. The irradiation geometry and parameters of the laser pulse remained constant during measurements. The light emitted from a plasma region located at a distance of  $\sim 200 \mu\text{m}$  from the target was detected in the direction perpendicular to the plume axis. Note that the dimensions and shape of the plume, which depended mainly on the laser-pulse intensity and pressure produced by the ambient gas [8], remained constant during their study as functions of the target composition. One of the tasks of this work was to study the effect of the target composition on the effective temperatures of a laser flash. An appreciable excess of the effective colour temperature ( $T_{\text{col}} \geq 5000 \text{ K}$ ) over the brightness temperature ( $T_{\text{br}} \leq 3000 \text{ K}$ ) determined experimentally in the visible wavelength region indicated that the plasma layer was optically thin. The absorption of radiation at frequencies of a line spectrum was also ignored, since the spectral lines usually selected for studies had low intensities corresponding to transitions of subordinate series.

In the analysis of the experimental dependences, we assumed that the target components were distributed uniformly over the plume volume and their relative densities in the evaporated substance remained constant as compared to their contents in the target. The fraction of free atoms in

the laser plasma was determined from the intensities of atomic line spectra.

## 3. Experimental results

### 3.1 Effect of pressure on the spectrum of the light flash

Figures 1 and 2 show the dependences of the intensity of the spectral lines for metals on the pressure of argon for copper and aluminium targets, respectively. The measurements were performed for the spectral lines of Cu (0.5105  $\mu\text{m}$ ) and Al (0.3961  $\mu\text{m}$ ) atoms and  $\text{Al}^+$  (0.4666  $\mu\text{m}$ ) ions.

As follows from Fig. 1, a linear rise in the intensity of the spectral line for Cu atoms [curve (1)] transforms into a saturation at a pressure  $p_a \sim 5 \text{ atm}$ . A different behaviour is observed for the intensity of continuous emission: a threshold character (at a percolation pressure  $p_{\text{per}} \sim 4 \times 10^{-1} \text{ atm}$ ) and a power-law increase in the intensity with a power index close to 1.75 [curve (2)] are clearly pronounced. Note that an abrupt drop in the intensity observed for all the spectra at pressures of  $> 10 \text{ atm}$  results, as follows from photography, from the fact that the plasma presses itself to the target surface [3, 8], so that its emission does not fall on the spectrometer slit.

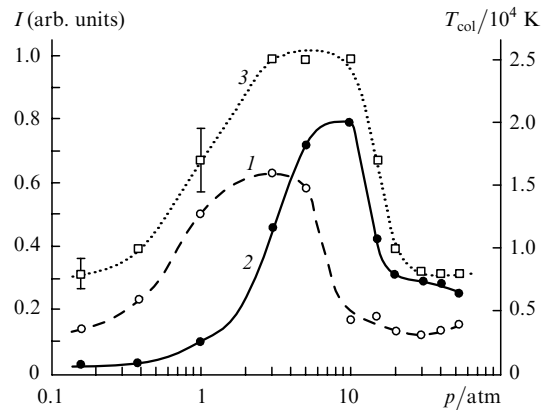


**Figure 1.** Effect of the pressure  $p$  of the ambient gas on the emission intensity  $I$  of the atomic Cu spectrum [curve (1)] and the emission continuum (2) in the laser plasma near the Cu-target surface and on the effective colour temperature  $T_{\text{col}}$  (3).

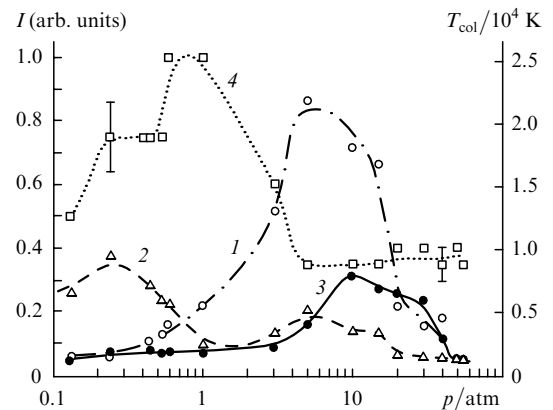


**Figure 2.** Effect of the pressure  $p$  of the ambient gas on the emission intensity  $I$  of the atomic [curve (1)] and ion (2) Al spectra and the emission continuum (3) in the laser plasma near the Al-target surface, and also on the effective colour temperature  $T_{\text{col}}$  (4).

For a spectral line belonging to singly charged Al ions, the peak intensity is observed at  $p_i \sim 3 \times 10^{-1}$  atm, which is ten times lower than for the atomic Al spectrum (Fig. 2). It is of interest that, in the pressure range  $10^{-3} - 3 \times 10^{-1}$  atm, the  $\text{Al}^+$  spectral lines broaden by a factor of  $\sim 3$ . It is known that the ionisation of a saturated vapour increases the nucleation rate by several orders of magnitude. Surrounding themselves by polarised vapour atoms, ions form bound structures. At low pressures, these are complex ions that are coupled due to a long-range interaction; at higher pressures, these are cluster ions ( $\text{Al}_n^+$ ) with valence bonds between ions and atoms [12]. The formation of complex ions occurring at pressures  $p < p_i$  is a probable explanation for the broadening of ion lines, and the formation of cluster ions accounts for a drop in the intensity of the ion spectrum at  $p > p_i$ .

Figure 3 shows the dependences obtained for near-surface plasma of a  $\text{Cu}_{0.5}\text{Al}_{0.5}$  binary target. Alloys have the following typical feature: copper atoms that are present in plasma have no effect on the concentration of complex Al ions at low pressures but prevent the formation of cluster Al ions. As a result, the region of the fall of the ion-spectrum intensity shifts to pressures  $p > 10p_i$ .

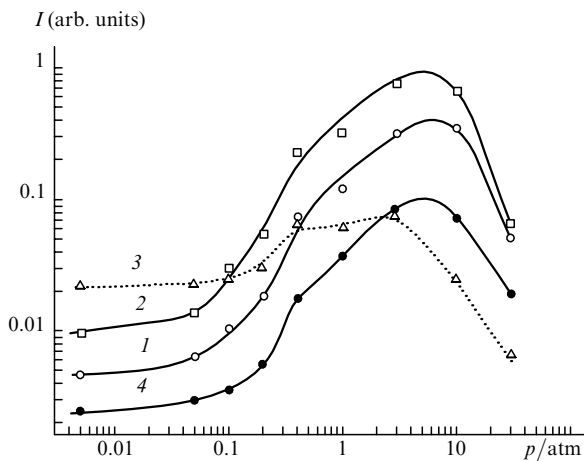


**Figure 3.** Effect of the pressure  $p$  of the ambient gas on the emission intensity  $I$  of the spectral lines of various laser-plasma components near the surface of a binary target: Cu [ $\lambda = 0.5105 \mu\text{m}$ , curve (1)] and Al [ $\lambda = 0.3961 \mu\text{m}$ , (2)] atoms and singly charged aluminium ions  $\text{Al}^+$  [ $\lambda = 0.4666 \mu\text{m}$ , (3)] in the laser plasma near the Al-target surface, and also on the effective colour temperature  $T_{\text{col}}$  (4).

When radiation is not absorbed, the spectral line intensity must be proportional to the density of the corresponding component in the plume volume, if the line width and profile do not change significantly. The widths of the atomic spectral lines of the metals under study are really independent of either the target composition or the buffer-gas pressure. The half-height line widths for Al and Cu are  $1.3 \pm 0.2$  and  $0.5 \pm 0.05$  nm, respectively. A natural assumption is that the saturation of atomic spectra at the moment of action of a laser pulse, when the peak intensity of spectral lines is emitted, is a consequence of a limited density of the number of free atoms in the plasma plume due to the formation of bound structures—clusters. Since the model of compact clusters does not correspond to a rather high gas plasma temperature ( $\sim 1$  eV [8]), gaslike [6] and percolation clusters are more suitable candidates for the role of ‘hot’ bound structures.

### 3.2 Effective emission temperature

Figures 1 and 2 also show the pressure dependences of the colour temperature  $T_{\text{col}}$  of plasma emission, which was determined by comparing the frequency dependences of the continuum observed in the experiment and of the black-body radiation. The emission intensity at the frequencies in the visible region cannot be described by a single brightness temperature  $T_{\text{br}}$ , if  $T_{\text{br}} \neq T_{\text{col}}$ . An inverse proportionality between  $T_{\text{br}}$  and the wavelength observed in the experiments for all of the targets under study agrees well with the model of Planck emission from an optically thin plasma layer, whose emissivity is frequency independent.

It follows from Figs 1 and 2 that the effective colour temperature of a light flash reaches a maximum at pressures of  $\sim 7$  and  $\sim 1$  atm for Cu and Al targets, respectively. It was determined in [3] that, for a millisecond laser pulse, the characteristics of radiation emitted by a laser plume depend on the electronic configuration of the outer shell of target’s atoms: as the temperature changes, there is a similarity in the behaviour of the plasma temperature near the surfaces of targets whose atoms belong to one and the same subgroup of the Mendeleev periodic table. Figure 4 shows the dependences of the effective colour and brightness temperatures ( $\lambda = 0.6 \mu\text{m}$ ) on the buffer-gas pressure obtained during the ablation of various metals irradiated by nanosecond laser pulses. The curves are presented for pairs of metals from a common subgroup. Their comparison confirms a conclusion from [3] that the electronic structure of the target’s atoms determines the effective colour temperature and its pressure dependence. For example, the maximum temperature  $T_{\text{col}}$  for rare-earth elements turns out to be several times higher than for elements from the group of iron. Note that a drop in the effective temperatures at pressures of  $> 10$  atm corresponds to the passage of the leading edge of plasma through the region, whose emission is detected by the spectrometer.

### 3.3 Effect of the target composition on the light-flash spectrum

The behaviour of the intensity of the spectral lines mentioned above was studied during ablation of Cu–Al binary alloys. Figure 5 shows the intensities of the atomic and ion spectra as functions of the composition of a  $\text{Cu}_x\text{Al}_{1-x}$  target. The experimental data were obtained at normal pressure of argon. As was mentioned above, changes in the widths of the spectral lines can be ignored when analysing the experimental results. It follows from Fig. 5 that a proportionality between the intensity of a spectral line and the density of the corresponding plasma component is violated when the relative atomic density begins to exceed  $n_a = 0.1 \pm 0.02$  and  $0.23 \pm 0.04$  for Cu and Al, respectively. These values are close to a value of  $\sim 0.15$  for the percolation threshold in the three-dimensional case [13]. Similar dependences of the spectral intensities on the target composition were obtained for a Cu:Ni target with a percolation threshold for Ni  $n_a = 0.16 \pm 0.02$ . The features observed in the behaviour of the intensities of the atomic spectra (Fig. 5) result from the limitation of the density of free atoms in the plasma plume due to the formation of percolation clusters consisting of atoms of a single metal.

Of interest is to compare the dependences obtained of the atomic and ion Al spectra. The ratio of the intensities of these spectra is a certain function of the atomic Al density in the plasma plume. Estimates based on the Saha equation for

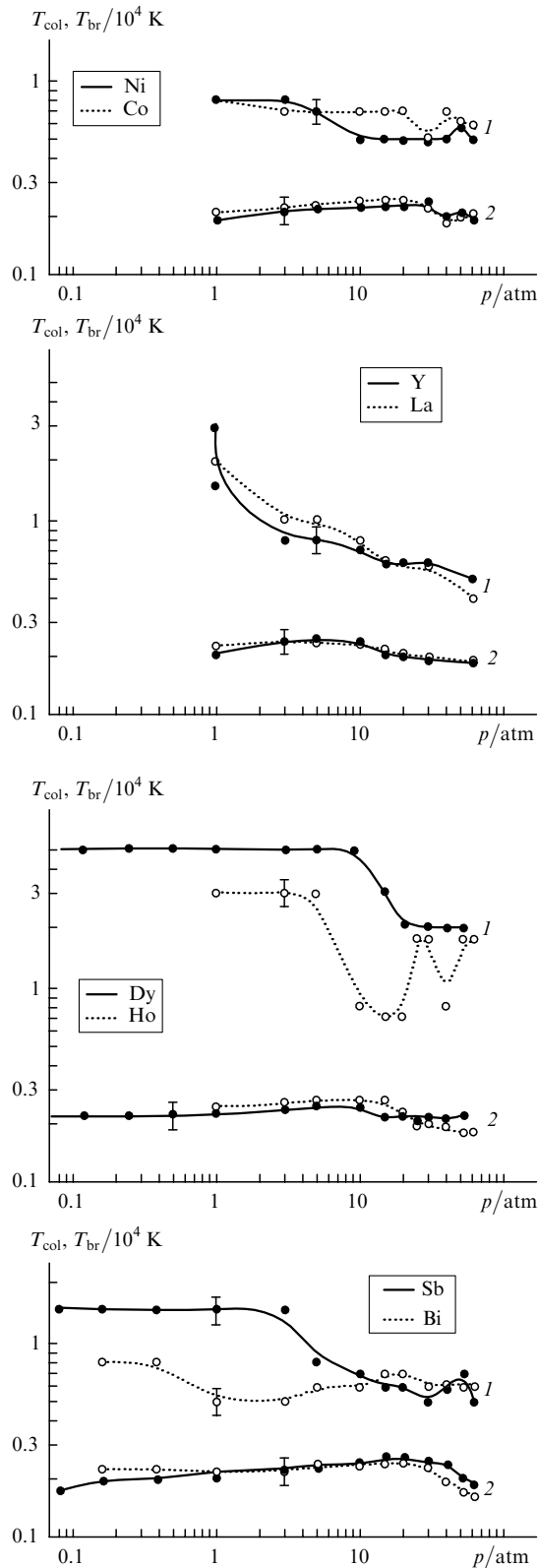


**Figure 4.** Pressure dependences of the effective colour [curve (1)] and brightness (2) temperatures of the near-surface laser plasma for metals from different subgroups of the periodic table.

ionisation equilibrium do not describe the behaviour of this ratio, if the effective flash colour temperature, the corresponding dependence of which is also shown in Fig. 5, is used as the plasma temperature. We assume that  $Al^+$  ions are trapped by a copper percolation cluster with a higher

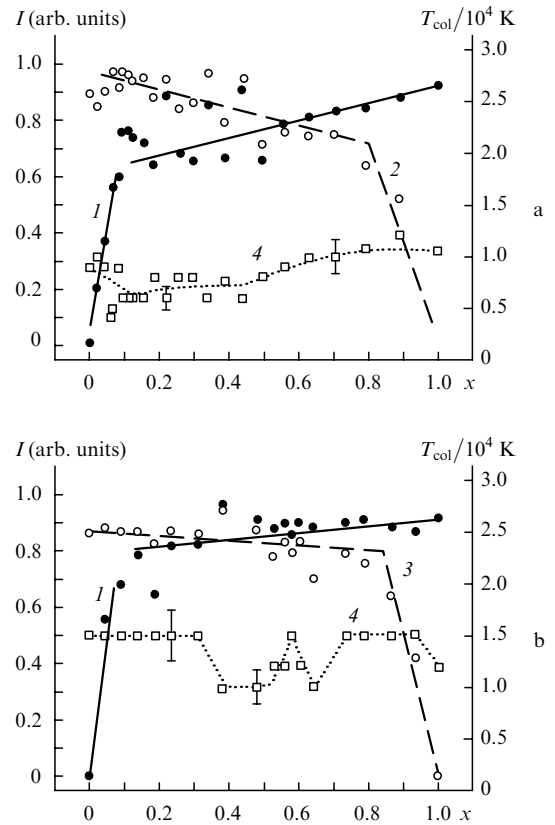


**Figure 5.** Behaviour of the intensities of spectral lines  $I$  [curves (1)–(3)] and the effective flash colour temperature  $T_{col}$  (4) as a function of the target composition at normal pressure of the buffer gas [ $Cu_xAl_{1-x}$  alloy in Ar (a) and  $Cu_xNi_{1-x}$  alloy in air (b)]: Cu [ $\lambda = 0.5105 \mu m$ , (1)], Al ( $\lambda = 0.3964 \mu m$ , (2)), and Ni [ $\lambda = 0.5477 \mu m$ , (3)] atoms.

probability than Al atoms. As a result, the density of free ions falls, as the density of Cu atoms increases.

During ablation of binary metal targets (both alloys and powder mixtures), a percolation threshold exists for each separate component and virtually has no effect on the other component. For a mixture of a metal and a salt, in addition to continuum and individual lines of the metal, the atomic spectrum of the metal included in the salt molecules is also observed. The peak intensities of the lines in Al and salt-metal spectra correspond to the relative atomic density  $n_a \sim 0.3$  (Fig. 6). This value is approximately 50% higher than the percolation threshold  $n_a$  for Al in a binary metal mixture. A possible cause for this difference is a decrease in the number of free Al atoms as a result of their participation in chemical reactions with the formation of fluorine compounds  $AlF_n$  ( $n \leq 3$ ) and liberation of the metal included in the salt molecules. In contrast to the results shown in Fig. 5, the intensity of the spectra in Fig. 6 considerably falls, when the percolation threshold is exceeded; this can be interpreted as a consequence of the fact that Al atoms, which were already included in the percolation cluster, do not participate in chemical reactions.

Note that, if the target is a powder mixture, it can be regarded as a medium for a three-dimensional percolation. However, the threshold in such an object is determined by the ratio of the volumes of the mixed substances but not by the atomic density [13]. The representation of the experimental results shown in Figs 5 and 6 as a function of the volume fractions of the target components leads to a much

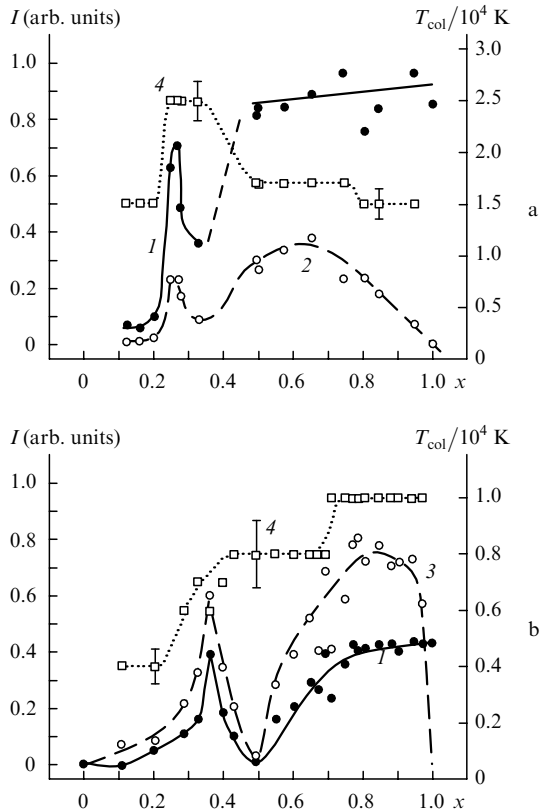


**Figure 6.** Behaviour of the intensities of spectral lines  $I$  [curves (1)–(3)] and the effective flash colour temperature  $T_{\text{col}}$  (4) as a function of the binary-target composition at an air pressure of 1 atm [ $\text{Al}_x(\text{LiF})_{1-x}$  (a) and  $\text{Al}_x(\text{MgF}_2)_{1-x}$  (b) powder mixtures]: Al [ $\lambda = 0.3964 \mu\text{m}$ , (1)], Li [ $\lambda = 0.4273 \mu\text{m}$ , (2)], and Mg [ $\lambda = 0.3838 \mu\text{m}$ , (3)] atoms.

larger difference between the thresholds (e.g., for copper) when changing from an alloy with Al to an alloy with Ni. In addition, the buffer-gas pressure does not affect the percolation in targets. An alternative model of ‘hot’ structures in a dense vapour is a model of a gaslike cluster with a minimum number of bonds between atoms [6]. At sufficiently high temperatures, such a structure takes the form of spontaneously appearing chains of atoms (virtual chains). Since the critical density for the formation of one-dimensional structures—the percolation threshold—approaches unity, this model does not comply with the experimental data of this study. The same argument also contradicts the model of a two-phase cluster [14], in which the outer monolayer of a compact cluster consists of particles with a small number of bonds. A percolation in a two-dimensional layer is characterised by a threshold equal to 0.5. In [15], a generalised model of virtual chains was proposed, within the framework of which a cluster in the form of a fractal-like system of coupled atomic chains has a topology very close to that of a percolation cluster.

#### 4. Conclusions

The studies performed in this work have shown that three-dimensional percolation clusters exist in the plasma produced upon ablation of targets into the ambient gas produced by nanosecond laser pulses. The percolation threshold is the critical atomic density of the evaporated target component. ‘Hot’ percolation clusters determine the

absorbability, temperature, and spectral continuum of plasma emission. The dependences of the continuum intensity and percolation threshold on the electron structure of target atoms indicate the presence of chemical bonds between structural elements of the percolation cluster. The question of the characteristic scale of a region in the laser plume, for which the microscopic percolation model is applicable [16], requires an additional study.

**Acknowledgements.** This work was partially supported by the Russian Foundation for Basic Research (Grant No. 03-02-17026) and the program ‘Scientific schools’ (Grant No. 1771-2003.2).

#### References

1. Goncharov V.K., Kontsevoi V.L., Puzyrev M.V. *Kvantovaya Elektron.*, **22**, 249 (1995) [*Quantum Electron.*, **25**, 232 (1995)].
2. Goncharov V.K., Puzyrev M.V. *Kvantovaya Elektron.*, **24**, 329 (1997) [*Quantum Electron.*, **27**, 319 (1997)].
3. Kask N.E., Michurin S.V., Fedorov G.M. *Kvantovaya Elektron.*, **34**, 524 (2004) [*Quantum Electron.*, **34**, 524 (2004)].
4. Kask N.E., Leksina E.G., Michurin S.V., Fedorov G.M., Choporniyak D.V. *Kvantovaya Elektron.*, **32**, 437 (2002) [*Quantum Electron.*, **32**, 437 (2002)].
5. Kask N.E., Michurin S.V., Fedorov G.M. *Zh. Eksp. Teor. Fiz.*, **116**, 1979 (1999).
6. Zhukhovitskii D.I. *Zh. Eksp. Teor. Fiz.*, **113**, 181 (1998).
7. Kask N.E. *Pisma Zh. Eksp. Teor. Fiz.*, **60**, 204 (1994).
8. Harilal S.S., Bindhu C.V., Tillack M.S., et al. *J. Appl. Phys.*, **93**, 2380 (2003).
9. Tillack M.S., Blair D.W., Harilal S.S. *Nanotechnology*, **15**, 390 (2004).
10. Panchenko A.N., Tarasenko V.F., Tkachev A.N., Yakovlenko S.I. *Laser Phys.*, **3**, 844 (1993).
11. Arepalli S., Nicolaev P., Holmes W., Scott C.D. *Appl. Phys. A*, **70**, 125 (1999).
12. Smirnov B.M. *Usp. Fiz. Nauk*, **121**, 231 (1977).
13. Shklovskii B.I., Efros A.A. *Elektronnyye svoystva legirovannykh poluprovodnikov* (Electron Properties of Doped Semiconductors) (Moscow: Nauka, 1979).
14. Zhukhovitskii D.I. *Zh. Eksp. Teor. Fiz.*, **121**, 396 (2002).
15. Zhukhovitskii D.I. *Zh. Fiz. Khim.*, **75**, 1157 (2001).
16. Likal'ter A.A. *Usp. Fiz. Nauk*, **162**, 119 (1992).